ISSN 1063-7729, Astronomy Reports, 2006, Vol. 50, No. 12, pp. 1013–1025. © Pleiades Publishing, Inc., 2006.
Original Russian Text © A.N. Shakhovskaya, M.A. Livshits, I.M. Chertok, 2006, published in Astronomicheskiĭ Zhurnal, 2006, Vol. 83, No. 12, pp. 1128–1141.

The Role of Plasma Ejections in the Development of Large Solar Flares of Various Durations

A. N. Shakhovskaya[1], M. A. Livshits[2], and I. M. Chertok[2]

[1]*Crimean Astrophysical Observatory, National Academy of Sciences of Ukraine, Nauchnyĭ, Crimea, 334413 Ukraine*

[2]*Pushkov Institute of Terrestrial Magnetism, Ionosphere, and Radiowave Propagation, Russian Academy of Sciences, Troitsk, Moscow oblast, 142190 Russia*

Received May 15, 2006; in final form, July 7, 2006

Abstract—Recent observations indicate that relatively strong plasma ejections are accompanied by the formation of systems of coronal loops with two glowing ribbons near their footpoints. However, while two-ribbon flares can sometimes last for many hours, for example, soft X rays, they sometimes decay within tens of minutes. We study here factors affecting the durations of flares using four major flares occurring in July 15–18, 2002, as examples. Various ground-based and satellite observations are used to show that short-duration events involved collimated (narrow) plasma ejections directed to the north and the subsequent formation of compact loops in the leading part of the active region. During one event, a powerful eastward ejection in a wide solid angle was followed by the formation of an extended arch system in the trailing part, which determined the long duration of the flare. It is proposed that in events involving collimated jets and corresponding narrow features in coronal mass ejections (CMEs), systems of coronal loops do form, but post-eruptive energy release either does not occur or is expressed very faintly. So the energy does not go downward from this region, and the plasma is emitted free in the coronal loops. In contrast to such rapid flares, wide ejections and bright, large-scale CMEs are accompanied by the formation and prolonged existence of an extended arch system. Thus, powerful nonstationary solar processes involve a large-scale CME and the flare itself, with the pattern of a particular event determined by the reconnection scenario and the evolution of the ejected plasma.

PACS numbers : 96.60.qe, 96.60.pf, 96.60.ph
DOI: 10.1134/S1063772906120067

1. INTRODUCTION

Solar flares can be divided into two classes with substantially different temporal emission profiles, spatial structure, and other parameters: rapid (compact) events and long-duration events (LDEs); see e.g., the review by Sakai and De Jager [1] and references therein. Analyses of prolonged observations of the solar soft X-ray emission with the GOES satellites indicate that these two classes of events can be distinguished even among powerful flares with X-ray classes higher than M5. In some cases, the X-ray burst appears as a narrow spike and is of a very short duration (from a few minutes to half an hour), while, in others, a fairly sharp peak is followed by a slow, many-hour decay. (Figs. 1a–1c).

Powerful phenomena were previously referred to as flares with complex spatial and temporal structure. Modern observational facilities make it possible to distinguish individual episodes in such flares, each consisting of an ejection (eruption) and the formation of a system of coronal loops filled with hot plasma. In some cases, there is free emission in dense flare loops after their formation. The emission times range from several to 20–30 min. For this reason, even if such events are powerful, they have very short durations. In many cases, they can be identified with compact flares [1, 2], whose Hα ribbons do not extend beyond relatively small active regions (smaller than 5′). In contrast, long-duration flares occur when powerful plasma ejections are accompanied by the formation of loops; in this case, either the loops persist for a long time due to additional plasma heating near their tops or newer loops form successively. In the final stage of such events, the entire system of posteruptive loops ascends, and a giant arch system forms.

Although many properties of rapid and long-duration events are known fairly well, the factors determining which flare scenario occurs remain unclear. General considerations suggest that an important role is played by the specific features of the magnetic configuration in the active region where the phenomenon develops. Moreover, the parame-

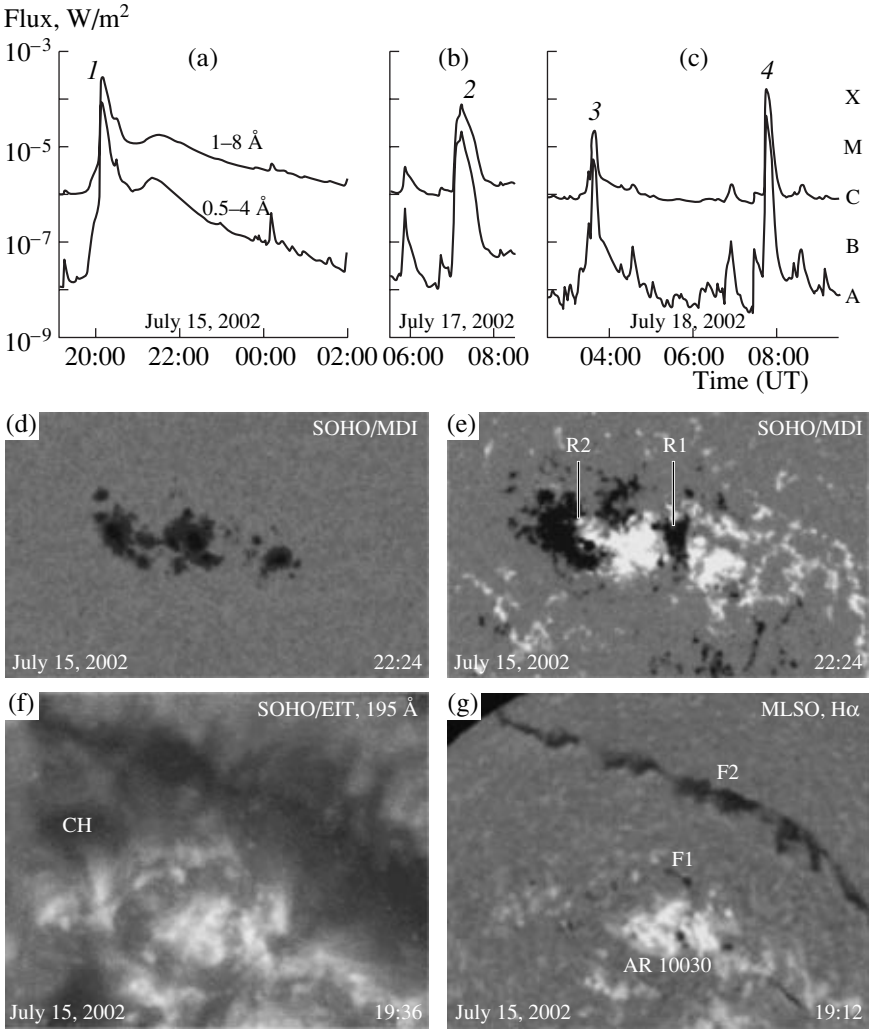

Fig. 1. (a–c) Time profiles of the flares of July 15–18, 2002, in the soft X rays according to GOES 8 data (table). (d, e) Sunspot group and the magnetogram of active region 10030 according to SOHO/MDI data (in the magnetogram, white and black correspond to northern and southern polarities). (f, g) Heliograms of a portion of the northern half-disk in the 195-Å channel (SOHO/EIT) and in Hα (Mauna Loa) illustrating the systems of bright large-scale coronal loops that stretch from the leading part of AR 10030 to the vicinity of the eastern coronal hole CH, the filament F1 that issues from region R1 and the extended filament F2 located in the high-latitude sector of the northern half-disk. The distance between the centers of large outermost spots is approximately 100″.

ters of the plasma ejection are important, since the ejection frequently results in an opening of loops during a coronal mass ejection (CME), the subsequent relaxation of the magnetic field to a new quasi-equilibrium state (a development of Kopp and Pneuman's ideas [3]; see [4] and references therein), and an additional energy supply to the upper part of the formed posteruptive loops.

We analyze here the role of plasma ejections in the subsequent development of flares—particularly, in providing conditions for the prolonged glow of the posteruptive loops—using the powerful flares of July 15–18, 2002, as examples. This sequence of flares included four events of classes M3 to X4.8 occurring in the same active region. A preliminary discussion of one of these, the event of July 18, was given in [5]. An intense ejection was coronagraphically observed at the Crimean Astrophysical Observatory (CrAO) during this event, after which the onset of a powerful posteruptive phase could be expected. However, this was not the case for that short-duration flare. It was suggested in [5] that the emergence of a dark ejection near the spot abruptly changed the development of the flare process, rapidly ceasing it. We analyze here the four most powerful events of this series from this point of view.

2. SOURCE DATA AND GENERAL CHARACTERIZATION OF ACTIVITY

Our starting point was an analysis of original observations carried out with the small CrAO coronagraph, described in [6–8]. This coronagraph makes it possible to obtain fairly frequent images of the solar disk or a selected active region at the center or wings of the Hα line, at an offset of about 1 Å with a time resolution of 1 s. This makes it possible to record ejections of interest. In contrast to previous observations, the images were recorded with a digital camera. In addition, we used some data obtained with the large CrAO coronagraph.

We also considered data on chromospheric activity obtained in the Hα line with the Big Bear and Mauna Loa ground-based telescopes (see ftp://ftp.bbso.njit.edu/pub/archive/ and http://mlso.hao.ucar.edu/cgi-bin/mlso_data.cgi?2002&ACOS) and in the 1600-Å band using the TRACE satellite [9]. The accompanying coronal phenomena were also studied using 171 and 195 Å TRACE observations (http://trace.lmsal.com/), and 195-Å observations with the SOHO/EIT EUV telescope [10] (http://umbra.nascom.nasa.gov/eit/eit-catalog.html). We used so-called fixed-base difference images along with original solar images [11, 12]. These can be obtained by compensating for the solar rotation and subtracting a pre-event, background image from all subsequent heliograms. We present also fixed-base difference image of CMEs obtained with the SOHO/LASCO white-light coronagraph [13] (http://cdaw.gsfc.nasa.gov/CME_list/; see the catalog of CMEs [14]). The properties of soft-X-ray flares were analyzed using GOES-8 data [15] (http://spidr.ngdc.noaa.gov/spidr/query.do?group=GOES&). We also used SOHO/MDI magnetograms [16] (http://soi.stanford.edu/data/). Below, we present only the most important illustrations. Additional data, such as images, heliograms, and computer movies can be found at http://www.crao.crimea.ua/shakhovskaya/july2002.html.

The table presents general characteristics of four major flares that occurred in AR 10030 (Carrington coordinates $N = 19$, $L = 012$) during the period from July 15–18, 2002 (see the site of the Solar-Geophysical Data, http://sgd.ngdc.noaa.gov/sgd/jsp/solarfront.jsp). We can see from the table and Figs. 1a–1c that, although in the soft X-ray range the three flares of July 17 and 18 had fairly high classes (from M2.2 to X1.8), they appeared as short pulses, and their durations at a level of one-fifth of the maximum were about 25, 12, and 11 min, respectively, i.e., the flares were rapid. Only in the most powerful flare of July 15 (class X3.0) had a similarly short pulse (17 min) followed by an additional component (class M3.8) with a slow decline in its emission, typical of LDEs, and with a duration of two to three hours.

It is important for our further analysis that the photospheric magnetic field in AR 10030 (Figs. 1d, 1e) had a complex $\beta\gamma\delta$ quadrupolar-type configuration, and the active region itself was strongly elongated in heliolongitude. In the leading (western) part of the region, an area of southern polarity (R1) was located between two large north-polarity spots, forming two relatively short neutral lines. The longer neutral line (R2) was located in the eastern part of the region, between the central, north-polarity spot and the trailing, south-polarity spot. During the passage of the region over the disk, many small, dynamically evolving spots and pores were observed in the vicinity of all three neutral lines; these formed freshly emerging magnetic fluxes. As the 195 Å heliogram (Fig. 1f) shows, the two western, north-polarity spots were linked by glowing coronal loops with a south-polarity trailing spot. In addition, some extended (high) UV loops stretched from the westernmost part of the region to the neighborhood of the eastern trailing spot and nearby coronal hole. The loop system between the leading and trailing spots was probably located over the Hα filament F1, which issued from AR 10030 in the northeastern direction (Fig. 1g). Note also that a very extended, large filament F2 was observed in Hα and the 195 Å UV channel to the north of AR 10030 and stretched from the equatorial part of the western limb to the northeastern limb.

3. RAPID FLARE OF JULY 18, 2002

We will begin our analysis of this series of rapid flares with the second, more powerful event on July 18 (No. 4 in the table). According to the 1600-Å TRACE observations, the flare began at 07:41[1)]; simultaneously, the GOES data indicate a sharp increase in the X-ray flux after a weak precursor at 07:20. The flux maximum in the GOES channels was reached at 07:44. The optical observations with the KG-1 coronagraph started at 07:42. In Hα, the flare developed in a regular way from 07:42 to 07:44; i.e., two bright flare loops ascended and the X-ray flux grew.

After 07:42, the powerful ejection 1 became appreciable at 1600 Å (Figs. 2a–2c). The ejected material appeared as a light ascending loop, whose footpoints were located in the northern parts of two flare ribbons. The material outflow continued nearly throughout the development period of this rapid flare. The speed

[1)]We indicate UT for all times.

Data for the events considered

No.	Date	Flare					Ejection				CME		
		t_0	t_m	d, min	Class	Coordinates	t_e	Type	Direction	V_j, km/s	t_c	Type	V_c, km/s
1	15.7.2002	20:02	20:08	17	3B/X3.0	N19 W01	20:03:27	NL	N	370			
							20:04:23	NL	N	700	20:30	PH+S	1150
		<21:03	21:32	>180	M3.8	–	20:24	WF	E	310	21:30	PH+S	1300
2	17.7.2002	07:00	07:13	25	1B/M8.5	N21 W17	07:17	NJ	N	190	07:31	PH+S	715
3	18.7.2002	03:22	03:37	12	SB/M2.2	N20 W27	03:38	LM	N–NE	–	no CME		
4	18.7.2002	07:38	07:44	11	2B/X1.8	N19 W30	07:42	NL	N	430	08:06	PH+S	1100

Note: t_0, t_m, and d are the beginning time, maximum time, and duration (at a level of one-fifth of the maximum) of the soft X-ray burst according to SGD data; t_e is the time of the main ejection phase. The ejection types are narrow loop (NL), wide front (WF), narrow jet (NJ), and plasma flow inside (along) a loop (LM). The ejection directions are northward (N), eastward (E), and northward with a change to northeastward (N–NE). V_j is the ejection speed, and t_c the time of the first LASCO/C2 observation of the CME. A CME of type PH+S is a partial halo with bright interior structures; V_c is the CME speed in the plane of the sky. We assumed that the time of the second microwave-burst peak corresponds to the ejection onset for event No. 3. UT is given for all time.

of the ejection front varied weakly; according to the 1600 Å observations, it reached a maximum value of 430 km/s.

This ejection became observable after 07:45 in Hα (Figs. 2d, 2e) as the narrow, dark feature 2. At nearly the same time, the X-ray flux of the flare and the Hα and 1600 Å brightnesses of the ribbons began to decrease abruptly. According to the Hα observations, the ejection extended northward until 07:51, remaining elongated and narrow; this extention terminated after 07:51, and the ejection began to split in a fanlike manner, into two and then four parts, also becoming darker at its northern end. After 08:05, the ejection slowly started to grow fainter, without changing its shape. By the end of the KG-1 observations at 09:05, the ejection was virtually indiscernible. The ejection was visible in the 195 Å SOHO/EIT images at 08:00 and 08:12. Here, it was also dark and closely resembled the structure of high coronal arches. The ejection arcs diverged, forming a fanlike pattern from AR 10030 to the north and reached the channel of the polar filament F2.

At 08:06, KG-1 filtergrams were obtained in the Hα wings at blue and red offsets of 0.5 Å. The ejection was well defined in the wings, with its area being much larger in the red than in the blue wing. The line structure of the ejection—its splitting into three or four meridionally stretched strips—was more clearly distinguishable in the red wing than in the line center. We constructed a difference image by superposing the blue- and red-wing filtergrams, taking a negative in the red and a positive in the blue wing. The difference is shown in Fig. 2f for time 08:06; the dark areas correspond to material upflow and the light areas to downflow. This means that the dark surge visible in the Hα mainly consists of upflowing material.

The observed low-temperature ejection was fairly powerful. In particular, even in the final stage of the development of the flare, no low-lying parts of the flare were visible through this ejection at the Hα center. This time, 07:55, corresponds to the time when the ejection became dark in Hα and transparent in 1600 Å. This demonstrative example of absorption is shown in Fig. 3, where the entire chromospheric flare is visible at 1600 Å through the low-temperature ejection, while part of the flare is obscured at the Hα center. It is possible that the low-lying loop linking the two loops was located in this obscured region. A spectrum obtained near Hα by A.N. Babin and A.N. Koval' with the CrAO large coronagraph indicates that fast (about 100 km/s) upflows were observed at one of the footpoints of this loop, in the sunspot penumbra, and a slow (about 5 km/s) downflow at the other [5]. It is probably in this low-lying loop that the main high-energy events occurred. In the case under consideration, the ejection probably disrupted the normal development of the flare and prevented the propagation of the process along the neutral line in the northeastern direction.

The fact that this ejection disrupted the development of the flare can be inferred from a hysteresis diagram of the logarithm of the temperature versus half the logarithm of the emission measure, $\log T$ vs. $1/2 \log \mathrm{EM}$. The diagrams in Fig. 4 were constructed using data of two X-ray channels of the GOES-8 satellite taken every minute. The points describe

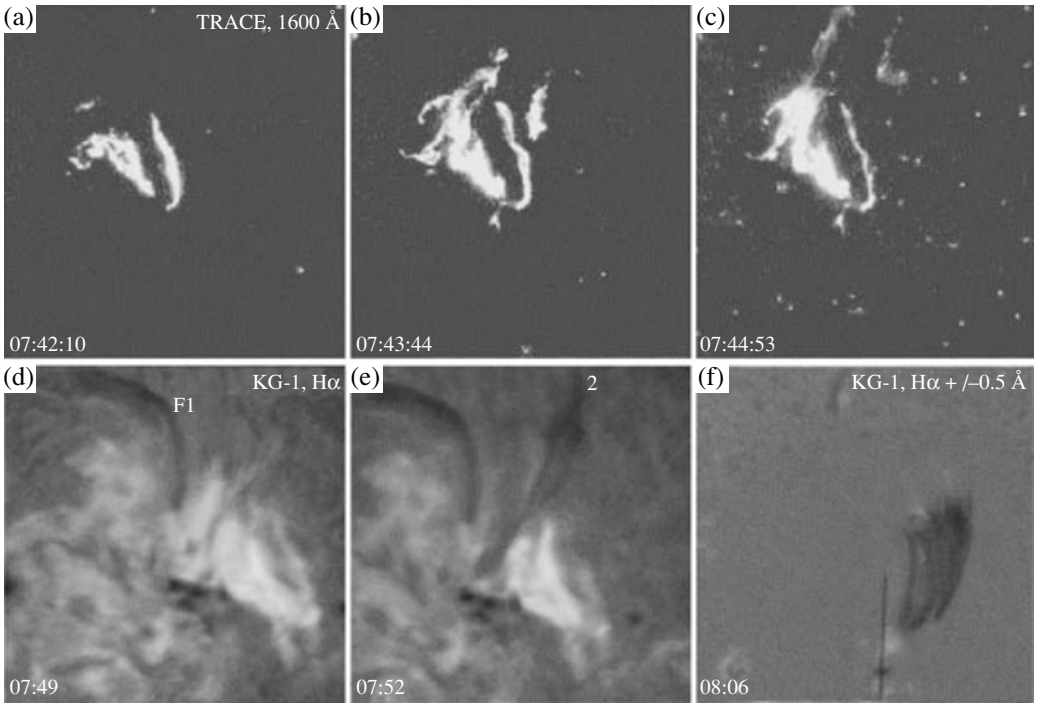

Fig. 2. Development of a collimated ejection in the rapid event of July 18, 2002 (No. 4) (a–c) at 1600 Å according to TRACE data and (d, e) in Hα according to the KG-1 coronagraph data. Diagram (f) presents a difference Dopplergram of the ejection in the blue (dark regions) and red (light region) Hα wings; the slit position of the CrAO large coronagraph is also indicated.

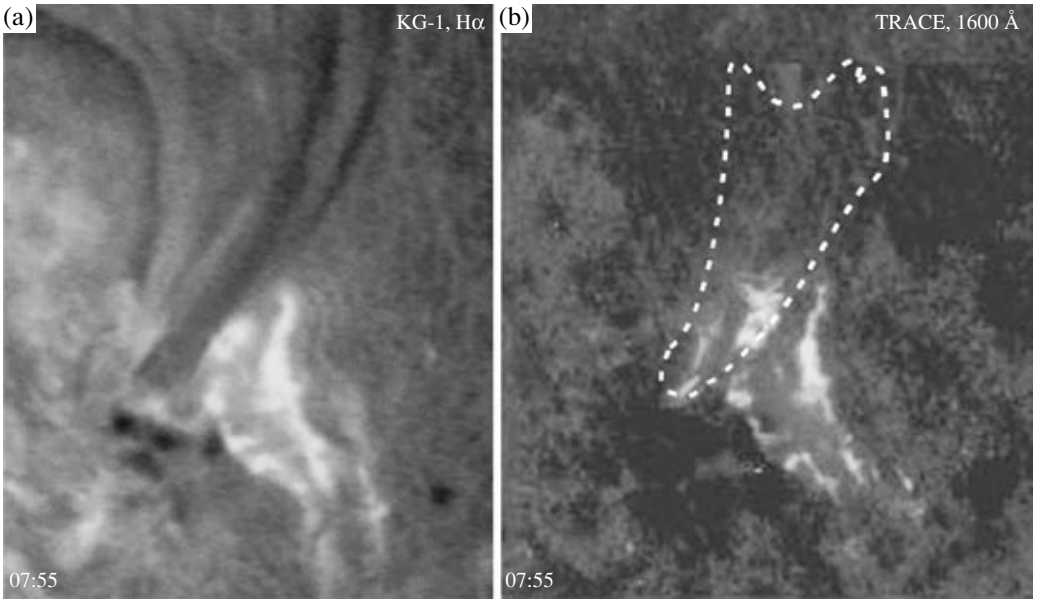

Fig. 3. Two-ribbon flare of July 18, 2002 (No. 4) in (a) Hα and (b) the 1600-Å channel with the contour of the Hα ejection at the line center superposed (dashed curve).

the temporal behavior of the thermodynamic parameters of the soft-X-ray source as a whole. For flare No. 4, the ejection went into the lower corona at 07:43 (heights from 10 to 20 Mm; see Fig. 2b), and the onset of posteruptive energy release (presumably, in the current sheet) was expected; in contrast, the development of the flare terminated abruptly (Fig. 4d). Normally, the decay phase lasts several hours rather than several minutes, as in this case. After 07:45, rapid radiative cooling of the plasma occurs in the

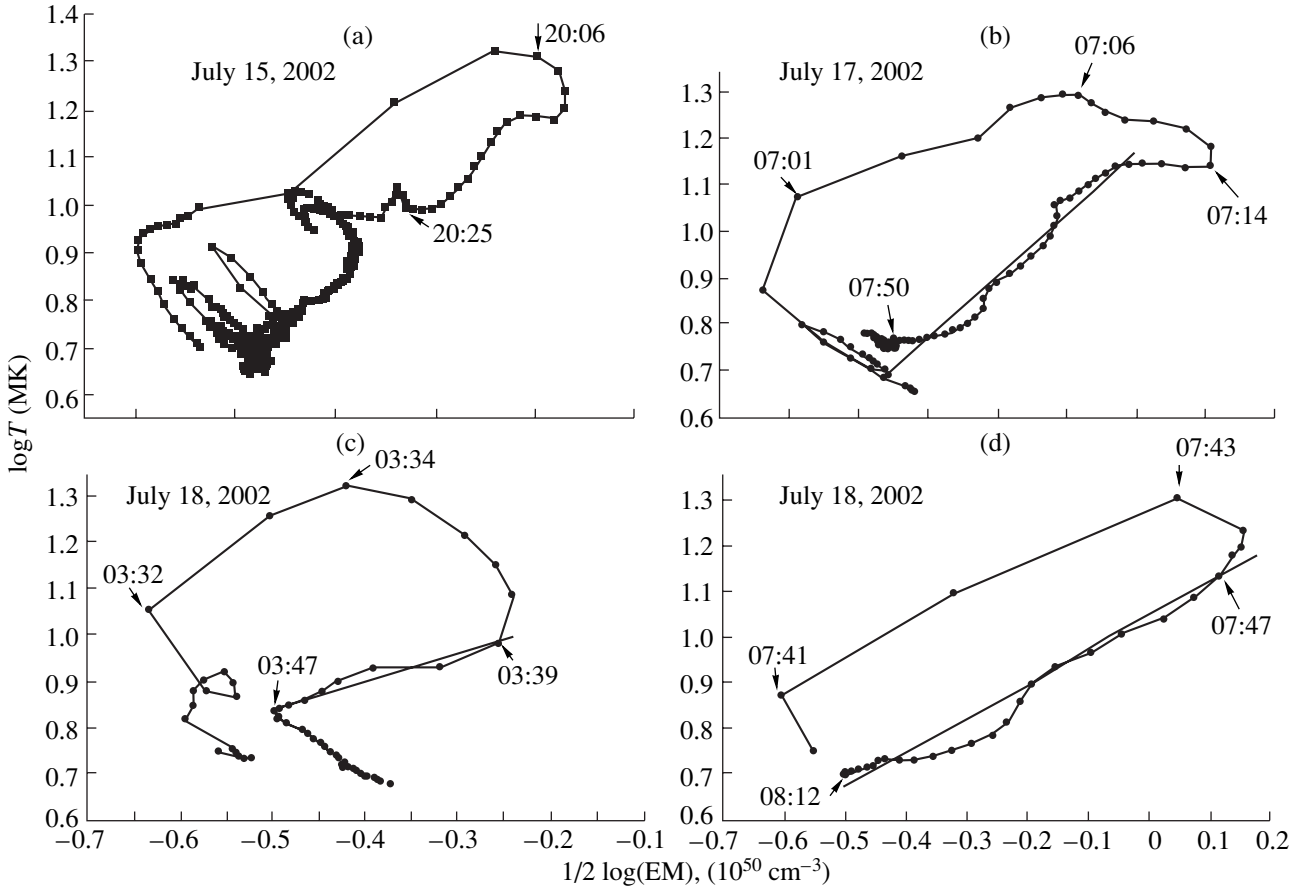

Fig. 4. Hysteresis $\log T - 1/2 \log EM$ diagrams based on the 1-min data of the GOES-8 X-ray channels for (a) the event of July 15, 2002 (no. 1) with a rapid and a prolonged component and (b–d) the rapid flares (nos. 2–4) of July 17 and 18, 2002. The times of some characteristic stages in the development of the events are marked.

coronal loops. We also note that the initial phase of the ejection coincided in time with a short-duration (a few minutes long) impulsive microwave burst with a radio-flux maximum at 07:43 at 9–15 GHz.

The LASCO data show that a multicomponent CME was associated with this flare, observed starting at 08:06. In the difference images (Fig. 5d), it appeared as a partial halo with a relatively faint flux around the whole northern half of the occulting disk of the coronagraph and included bright internal structures of small angular sizes over the northern limb. According to the catalog of CMEs, the eruption of this CME is close in time to the ejection described above, and the mean northward velocity of its front is ≈1100 km/s. Based on the parameters of the observed disturbances, it is reasonable to suppose that the bright narrow CME structures over the northern limb correspond to the ejection that was observed in Hα and the 1600 Å band. The faint halo was related both to the eruption of high and extended coronal structures itself and to the propagation of matter toward the observer. In particular, the fixed-base difference SOHO/EIT images in the 195-Å channel suggest that such structures erupted (Fig. 6b). Here, these erupted structures can be seen as dark, long-lived (persisting for several hours) dimmings formed at the sites of the pre-event bright structures. In particular, we can distinguish dimmings corresponding to the outer parts of the loop system, between the leading and trailing regions of AR 10030 and between the leading part of this region and the neighborhood of the coronal hole. Moreover, the extensive polar dimming indicates the eruption of loops stretching over the extended northern filament F2 and linking AR 10030 with the northern polar region (Figs. 1f, 1g).

It is important that, according to chromospheric (Hα and 1600 Å) and lower-corona (171 and 195 Å) data, the site of this flare (element 3 in Fig. 6b) was located in the leading part of AR 10030 (region R1 in Fig. 1e), where there is an incursion of southern-polarity field between the two north-polarity spots, and did not affect the trailing part of the region.

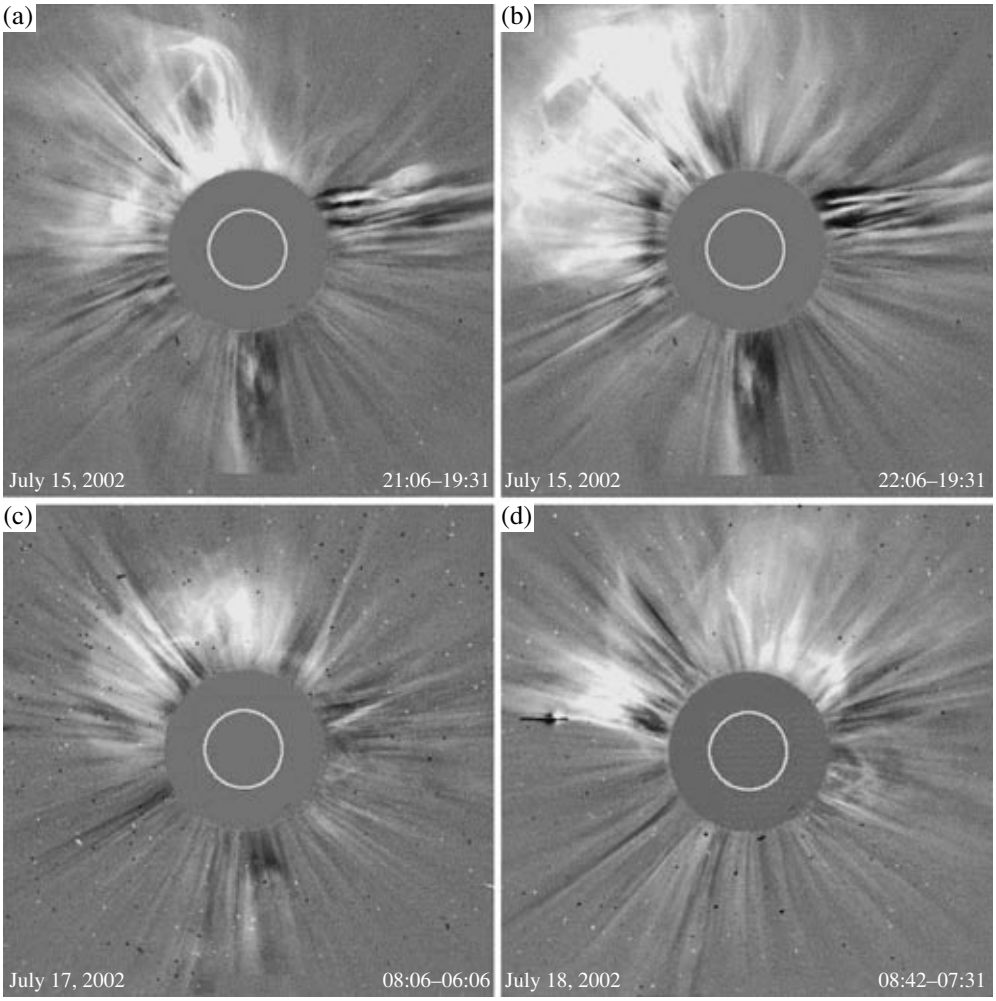

Fig. 5. Fixed-base difference images obtained with the SOHO/LASCO/C2 coronagraph illustrating a partial-halo CME over the northern limb sector with bright elements of internal structure corresponding to chromospheric ejections, in events No. 1 (two CMEs), No. 3, and No. 4 of July 15, 17, and 18, 2002.

4. OTHER RAPID EVENTS

Two other rapid flares, on July 17 and in the morning of July 18 (No. 2 and No. 3 in the table) originated and developed at the same place in the active region as event No. 4. Our comparison of the MDI magnetograms and 195 Å images for events No. 2 and No. 3 shows that the cores of these flares and the sources of the ejections were again located in the leading part of the active region, east of the first spot (region R1 in Fig. 1e), i.e., at the site where the ejection originated in event No. 4.

In soft X-ray emission, flare No. 2 had a bell-shaped time profile with a maximum at 07:13 (Fig. 1b). Its duration (25 min) slightly exceeded that of flare No. 4; however, the growth and decline of the emission were fairly sharp, so that this flare, by and large, should also be classified as rapid. At centimeter wavelengths, flare No. 2 was recorded as a two-component impulsive burst with comparable radio-flux maxima at 07:03 and 07:13. The frequency spectrum of the second pulse was harder (contained higher frequencies) than that of the first pulse.

Both episodes of energy release in flare No. 2 were clearly visible in the chromospheric and coronal emission, e.g., in Hα, at 1600 Å and in the aggregation of lines in the 195 Å channel. After the first pulse, a compact two-ribbon flare developed near the middle of the three spots and lasted for about ten minutes. During its final stage, at 07:13, ejection 4 started developing, which was well defined at the end of one ribbon (Figs. 7a, 7b). In terms of many of its parameters, this ejection was similar to that observed in event No. 4, but is slightly weaker. Nevertheless, it affected not only the chromospheric layers but also the outer part of the system of high coronal loops visible in Fig. 7c. It originated at the same site, about 14 000 km northeastward of the original focus of the flare, and was also directed northward. At later

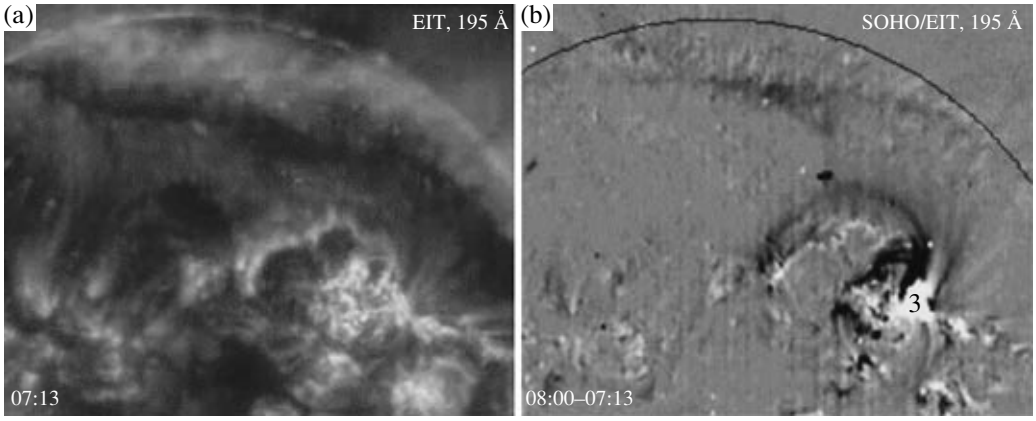

Fig. 6. (a) Original and (b) difference heliograms of the northern disk sector before and after the rapid event of July 18, 2002 (No. 4) in the SOHO/EIT 195 Å channel. The bright structure in the difference heliogram is the core of flare 3 in the western part of AR 10030 (region R1 in Fig. 1e), while the dark structures are large-scale CME-related dimmings.

times, the Hα observations show that the large-scale ejection formed a characteristic pattern of splitting into several strips, similar to that observed in event No. 4; the interaction of the ejection with the extended northern filament was also similar in these two cases. After this ejection, the glow of the coronal loops decayed rapidly. This could be due to both the weakness of the ejection and the violation of the conditions for magnetic-field-line reconnection in the current sheet.

As can be judged by the EIT difference heliograms in the 195-Å channel (Fig. 7c), the dimmings in this event involved virtually the same coronal structures as those in event No. 4. In particular, a substantial brightness decrease was observed over a large part of large-scale loops stretching from the zone of the leading spots (where the flare and ejection occurred) to the region of the trailing spot and the eastern coronal hole. Dimming disturbances are also seen in the difference movies representing the northern polar region (although to a lesser extent than in event No. 4); again, this is indicative of the eruption of large-scale loops located over the extended northern filament F2.

The CME that accompanied this flare also had much in common with the CME in event No. 4. It was first recorded by the LASCO/C2 coronagraph at 07:31, when the CME appeared over the north pole as a relatively small, fairly diffuse, loop-shaped structure. Over the following several tens of minutes (Fig. 5c), the CME brightness and size increased substantially, and the CME extended over the entire northeastern sector of the limb and acquired a partial-halo appearance with a number of bright internal features. According to the estimates given in the catalog, the mean speed of this CME was ≈715 km/s. As in event No. 4, the outer part of the halo seems to correspond to the eruption of high coronal structures, as is indicated by the large-scale UV dimmings observed in the 195 Å channel described above. However, the internal bright structures in the CME and, in particular, its brightest component over the north pole, most likely correspond to the plasma ejection from the western part of AR 10030 described above.

The rapid event of the morning of July 18—No. 3, with a soft X-ray maximum at 03:37—was a compact brightening of the same, relatively small area 3 in the western part of the active region, where impulsive energy release occurred during the preceding event, No. 2, and the subsequent rapid event, No. 4. This can be seen in the original EIT image in the 195-Å channel (Fig. 7f) and the corresponding chromospheric images. At later times (after 03 : 42), a compact two-ribbon flare was observed. Unfortunately, there are no data on the onset of the flare for this event, so that we could miss the initial ejection. At the same time, the material ejection recorded by TRACE after 03:42 seems to differ from the two cases considered above. A movie taken in the 195 Å channel shows that the propagation of the brightening along the first large-scale coronal loop (visible in Figs. 7c and 7f, in both the difference image for July 17 and the original image for July 18) was initially observed. This siphon-type motion was directed from the middle spot toward the northeast. Further, the brightening in the nearby large loop was observed to propagate in the opposite direction. We have the impression that, in contrast to the previous cases, the material was not ejected outward, but instead was redistributed within the high arch system. This agrees with the fact that no CME or large-scale dimming were present in the northern polar region in this case. At centimeter wavelengths, event No. 3 was recorded as a simple impulsive burst with a maximum at 03:33.

The effect of the ejections on the development of rapid processes in events No. 2 and No. 3 can also

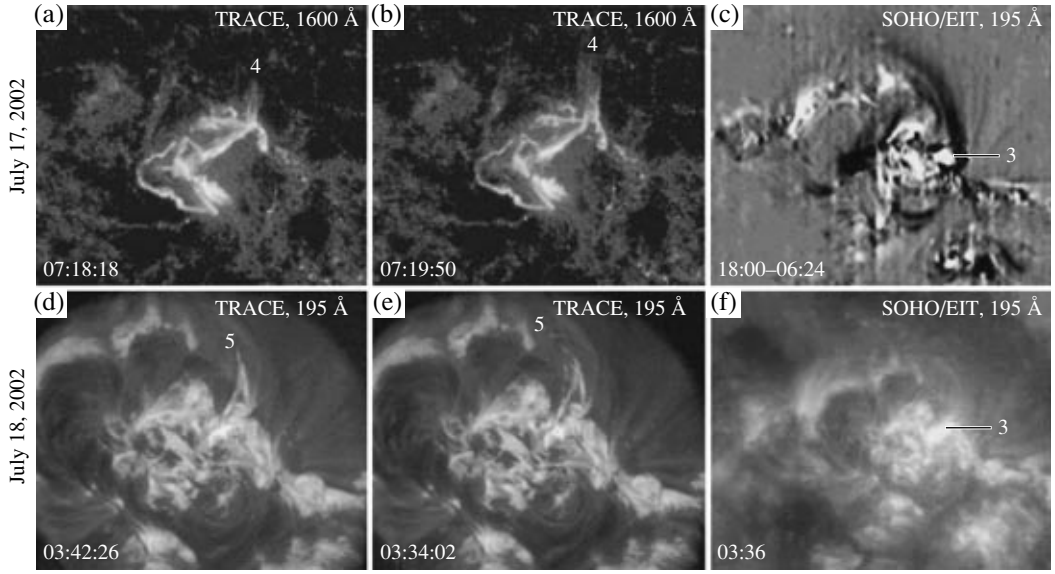

Fig. 7. Rapid events of July 17, 2002 (No. 2; top row of diagrams) and July 18, 2002 (No. 3; bottom row of diagrams). The collimated ejections 4 and 5 can be seen in the (a, b) 1600 Å and (d, e) 195 Å TRACE heliograms, respectively. The (c) difference and (f) original SOHO/EIT heliograms in the 195 Å channel show dark dimmings and the location of the bright core 3 of both flares in the western part of AR 10030 (region R1 in Fig. 1e).

be traced in the corresponding $\log T - 1/2 \log EM$ hysteresis diagrams. In event No. 2 (Fig. 4b), the development of the ejection in the final stage of the flare, at 07:17, resulted in the onset of the posteruptive phase of the event. This was similar to what occurred in event No. 4; however, in this case, the ejection disrupted only a portion of the coronal loop system, while the remaining loops continued glowing even with a small energy supply to their tops. The diagram for event No. 3 (Fig. 4c) testifies to a coronal scenario of the flare. Nevertheless, even in this case, the development of the flare slowed dramatically at 03:38, after the second peak of the microwave emission presumably induced by the ejection. However, a portion of the loops that is probably located outside the active region continued glowing over a fairly long time after 03:47. According to Livshits and Badalyan [17], the difference in the slopes of the linear approximations in the decline stage of rapid events Nos. 2–4 depends on the degree to which radiative losses in the loops are compensated by heating by energy supplied from the source of the posteruptive process.

5. LONG-DURATION FLARE OF JULY 15

The earliest, long-duration flare of July 15 (No. 1) likely changed the magnetic configuration, creating the necessary conditions for the subsequent short, compact flares. This prolonged event of optical class 3B included three main ejections, a corresponding rapid component, and a subsequent posteruptive phase.

The initial rapid component observed at 20:00–20:03 consisted of several compact coronal loops. Like the other rapid flares considered above, it originated and developed in the western part of the region, where there was an incursion of field of southern polarity between two spots of northern polarity (region R1 in Fig. 1e). We followed the successive development of the episodes of this complex event mainly using 1600-Å TRACE movies, together with images in the short-wavelength CIV ion line [18]. The first ejection of material was observed after 20:03 at 1600 Å (table), with its speed reaching a maximum 370 km/s within 0.5 min. Later, this ejection was absorbed by the following one.

At 20:03:49, the large-scale motion around the main core of the flare gave rise to a large ejection in the northern direction. This can be seen from chromospheric data, e.g., at 1600 Å (Figs. 8a, 8d). The violent rotation of plasma was characteristic of the onset of this ejection 6. Later, the ejection started propagating toward the north, leading to the regular development of a compact, two-ribbon flare. One small ribbon included the core of flare 3, while the other was located to the east of it. The glow of these ribbons lasted over 15 min.

This powerful ejection included a spiral, ropelike feature (Fig. 8a). One end of the spiral ascended more rapidly than the other, and the speed reached 700 km/s as early as one minute after the formation of this feature. This ejection was discussed briefly in [19], and the ejection itself, the ejection scenario,

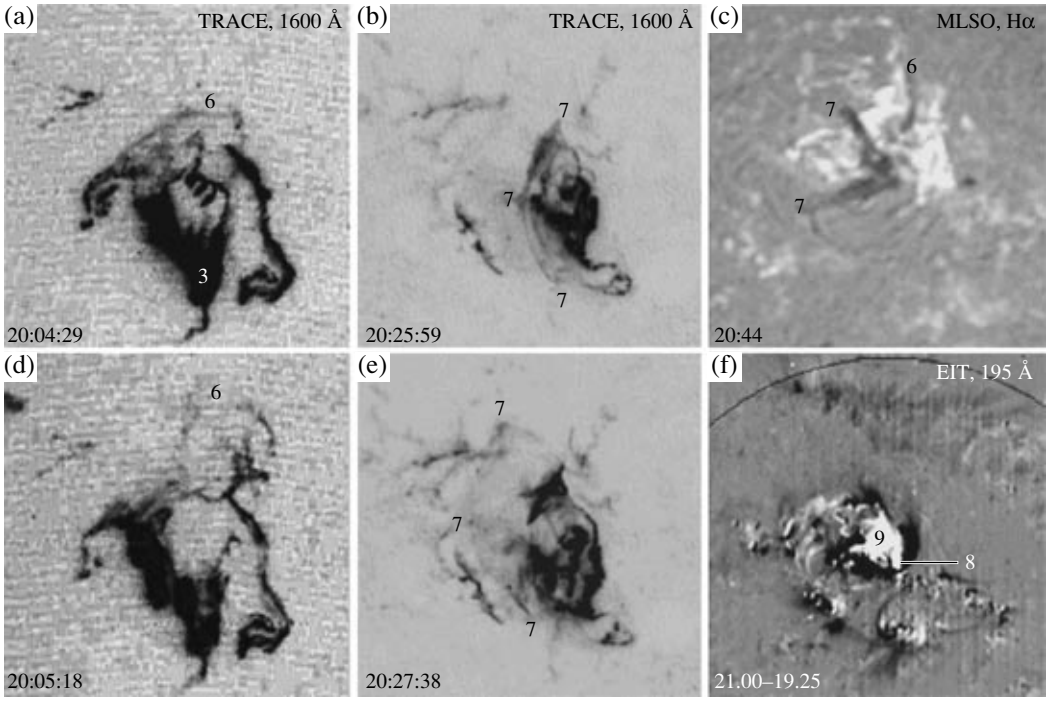

Fig. 8. Left-hand and central columns of diagrams: the development of (a, d) the collimated ejection 6 in the northern direction and (b, c) the wide ejection 7 in the eastern direction during the event of July 15, 2002 (No. 1) according to 1600 Å TRACE data (a negative). Right-hand columns of diagrams: appearance of these two ejections in (c) Hα according to data of the Mauna Loa observatory and (e) SOHO/EIT difference heliogram obtained in the 195-Å channel, which illustrates the dark dimmings and the location of the compact source of the rapid component 8 and of the extended posteruptive arcade 9 in the leading (area R1 in Fig. 1e) and trailing (area R2) portions of AR 10030, respectively.

and a model for the first part of the flare process are considered in more detail in [18, 20]. The time variations in the speed measured by us using the 1600-Å TRACE movie virtually coincides with the results obtained independently by Gary and Moore [18]. The parameters of the ejection were compared with relevant theoretical models of flares in [18, 20], and we will not dwell on this here. It is this ejection that gave rise to the first CME toward the north (with a speed of 1150 km/s; see the table).

Later (at 20:10), one more relatively weak, additional ejection traveled in the northern direction, after which another northern pair of ribbons was formed by 20:14–20:16. The impulsive part of the entire event essentially terminated by the end of this episode.

A new important event was established at 20:16 in the main core of the flare; by 20:23:30–20:24:30, it resulted in the development of another flash phase in the core of the flare and the onset of the powerful ejection 7 (Figs. 8b, 8e). In contrast to all the preceding ejections, this one traveled eastward. It is important that this ejection was not collimated, in contrast to those described above, and appeared as a large loop system encompassing a wide solid angle. Even in the initial stage, the ejection speed measured in the 1600-Å channel grew rapidly from 70 km/s at 20:25 to 310 km/s at 20:28.

We can compare the properties of the main ejections, 6 and 7. We can see from the table that the minimum observed speeds in the plane of the sky differ by more than a factor of two. However, this difference depends more on the orientation of the velocity vector with respect to the line of sight than on actual differences in the plasma velocities in these ejections. This follows from several reasons, in particular, the similarity of the velocities of the corresponding CMEs (1150 and 1300 km/s; see the table). In other words, all the ejections directed northward had larger projections onto the plane of the sky than the eastern ejection.

The large ejections 6 and 7 were visible in Hα (Fig. 8c). While all these rapid events left the quiescent filament located to the east of the flare core completely unaffected, the eastern ejection was probably a stream of fairly cool gas of this filament. The character of the absorption of the chromospheric emission in the 1600-Å and Hα filters—a rapid transition from sharp, dark loops to faint, more diffuse features—testifies

to a gradual increase in the temperature during the ejection process.

This activity was accompanied by two large successive partial-halo CMEs, which were loop-shaped and had several bright internal elements, with an emission maximum over the northeastern limb sector (Figs. 5a, 5b). The first of these CMEs was recorded beginning at 20:30, contained bright structures at its western flank (near the north pole), and ascended into the corona at a mean speed of 1150 km/s. The second, more intense CME became visible at 21:30, included several bright features distributed over the whole width of the loop-shaped transient and had a speed of 1300 km/s. The parameters of these two CMEs suggest that they are associated with the northern and eastern ejections, respectively. As for the UV dimmings related to these chromospheric ejections and CMEs, the difference image obtained in the 195-Å channel (Fig. 8f) shows substantial brightness decreases involving the immediate vicinity of AR 10030, the loop system stretching to the region of the eastern coronal hole, and structures located south of the active region and north of the extended filament F2. This means that the eruptive processes involved both local, inner (low-lying) structures constituting the magnetosphere of AR 10030 itself and structures of the global solar magnetosphere on much larger scales.

As a result of the large eastern ejection and the corresponding second CME, a large-scale system 9 of posteruptive loops on a relatively large scale (Fig. 8f), developed following the emergence of the core of the rapid component 8. An important difference of this loop system from all the rapid flares was that it was located over a relatively long magnetic-field neutral line in the eastern part of the active region, between the central spot of northern polarity and the trailing spot of southern polarity (area R2 in Fig. 1e). Just development of this posteruptive system causes the presence of the second, prolonged (LDE) component of the soft X-ray burst. The hysteresis diagram (Fig. 4a) shows that, while the ejection 6 (Figs. 8a, 8d) resulted in a virtual cessation of the flare process at 20:04, the loop system formed after ejection 7 (Figs. 8b, 8c), at 20:25, was characterized by a fairly large emission measure that persisted over several hours.

At centimeter wavelengths, the rapid and posteruptive stages of event No. 1 had parameters typical of such events. An intense two-component impulsive burst with a maximum at 20:04 and a hard (high-frequency) spectrum corresponded to the rapid component, and a prolonged burst with a lower intensity, a smooth time profile, and a soft (low-frequency) spectrum corresponded to the posteruptive component. Radio data for this event are discussed in [18].

6. DISCUSSION

The basic observational results if this study can be summarized as follows:

(1) All the rapid flares (events Nos. 2–4 and the impulsive component of event No. 1) occurred in the same area in the leading (western) part of AR 10030, where there was an incursion of field of southern polarity between two spots of northern polarity, and was accompanied by large, collimated (narrow) ejections of plasma in the northern direction. This demonstrates the homological behavior of these rapid events. In three of these cases, the ejections could be traced as narrow bright elements in the corresponding sectors of wide-angle CMEs related to the eruption of large-scale structures outside AR 10030.

(2) A prolonged LDE component with a long-lived posteruptive arcade localized over a relatively long neutral line in the trailing (eastern) part of AR 10030 occurred only in event No. 1, following a large-scale ejection. This ejection originated in the leading part of the region, as in the case of the rapid flares, but, in contrast to these, traveled toward the east within a wide cone that included the entire angular sector of the related bright large-scale CME.

The available observations suggest that, in an active region or activity complex, there is a small area (point) at the neutral line of the line-of-sight magnetic field where the basic high-energy phenomena develop [21]. By the energetic core of the flare, we usually mean the loop passing through this point nearly perpendicular to the neutral line. There are reasons to identify this line with the projection of the separator onto the photospheric surface. The reconnection process is probably most efficient precisely near the separator [4, 22].

Prolonged, LDE flares occur where conditions are created for the formation and development of a sufficiently long posteruptive loop system, in which either the existing loops are additionally heated or new loops filled with hot plasma are progressively formed over several hours. If the flare process reduces to a fairly intense primary energy release within a relatively small, spatially restricted area in the active region near the energetic core of the flare, the radiation generated in one or several loops without additional energy release is rapidly emitted, within a few tens of minutes, so that a rapid flare is realized.

An important role in determining the duration of flares is played by ejections. In the context of major flares, we use the word ejection (eruption) to denote a plasma outflow that can be observed in the lowest layers of the solar atmosphere and is gradually transformed into a CME. We should stipulate that this could be either an ejection of plasma with chromospheric temperatures, including the eruption of a

filament, or the ejection of dense coronal loops. Here, we will also include the impulsive phase in the concept of an ejection. Indeed, the explosive evaporation of plasma after the impact of accelerated electrons (or, in some cases, heat fluxes) on the chromospheric layers at the footpoints of the loops results in the emergence of an ascending flow of hot plasma at one or both loop footpoints. Normally, this hot gas fills the loop and does not go outside its volume. However, in some cases, e.g., if the number of accelerated electrons is large, the loop tears and plasma flows out. If the problem is formulated in this way, nearly any powerful ejection is accompanied by the formation of a system of coronal loops, which is manifest in the chromosphere as two ribbons. In a general, powerful nonstationary process, the large-scale ejection can result in the opening of field lines, as was suggested by Kopp and Pneuman [3]; during the subsequent relaxation, this can stimulate the process of posteruptive reconnection. Let us consider in which cases a loop system exists over many hours after the ejections, and in which cases the plasma emittance is lost immediately.

A posteruptive phase can be virtually absent, even in the case of a powerful ejection, if the ejection travels in a fairly small solid angle. This ensures the formation of coronal loops only within a restricted area over the neutral line. Current-sheet reconnection in the ejection region occurs over a short time, after which additional energy is not supplied to the coronal loops that have formed. For this reason, coronal loops do not form after the majority of such ejections and they radiate freely.

The ejections can disrupt the normal development of a two-ribbon flare and prevent it from changing into a long-duration event. The sharpest impact simply consists in the breakdown of the current-sheet region under the influence of another (external) ejection. The earliest interpretation of event No. 4 [5] was based precisely on the idea that the core of the flare was destroyed by an ejection that originated in low layers and had an appropriate orientation. Generally speaking, the emergence of a second ejection external to the flare can disrupt the normal development of the flare process. This situation could presumably be present during the two-ejection impulsive phase of the event of July 15, 2002 (table). However, much more frequently, the ejection disrupts the conditions for either the existence of the current sheet or the propagation of the process along the neutral line in both directions from the core of the flare.

Ejection in a wide solid angle can, however, result in the formation of a current sheet over a fairly extended section of the neutral line. This is possible if either a major flare has a powerful impulsive phase or the ejection of large filaments occurs without impulsive manifestations. In this case, if the formation of a CME is accompanied by the emergence of a large-scale current sheet (as can be seen, e.g., from the computations of [23]), an extended system of posteruptive loops develops at fairly low heights. Additional heating of the plasma confined in these loops due to energy supplied from the current sheet ensures the prolonged existence of the arcade over its whole extent.

Thus, the development of a long-duration flare occurs after a sufficiently powerful ejection in a wide solid angle. Narrow, collimated ejections result in the subsequent development of a system of coronal loops (and, accordingly, a two-ribbon structure at low heights); however, their lifetimes are short.

An additional factor that could play an important role for the development of long-lasting flares was considered by Livshits [24] in his analysis of energy and mass balance for the plasma contained in large-scale arch systems, based on CORONAS F data [25]. In particular, it was noted that the ejection and subsequent fall of material can play a large part in forming the posteruptive loops and ensuring their long lifetimes. Not only the amount of ejected plasma but also the gradual formation of a hot cloud of this plasma at large coronal heights prove to be important. The subsequent fall of material to the region of closed field lines—in particular, over magnetic-field neutral lines—can sustain the prolonged existence of the posteruptive system and its soft X-ray emission. The reconnection of magnetic-field lines can then be important in the immediate vicinity of the flare core (near the spots), while the effect of falling material becomes predominant well away from the core.

Further investigation of rapid and long-duration flares requires a more detailed analysis of the roles of the configuration of the active region and its location relative to the polarity-separation line in the large-scale magnetic field.

ACKNOWLEDGMENTS

We are grateful to the SOHO/EIT, LASCO, MDI (SOHO is cooperative ESA–NASA project), TRACE, and GOES teams and to the staff of the Big Bear and Mauna Loa ground-based solar observatories for the data used in our analyses. We also thank V.V. Grechnev (Institute of Solar-Terrestrial Physics, Irkutsk) for the IDL programs used to construct the difference images, and to O.G. Badalyan (Pushkov Institute of Terrestrial Magnetism, Ionosphere, and Radiowave Propagation, Troitsk, Moscow region) for preparing the hysteresis diagrams. This work was supported by the Russian Foundation for Basic Research (project nos. 05-02-17105 and 06-02-16106), the Ministry of Education and Science of

the Russian Federation (grant NSh-7495.2006.2), the basic-research program of the Presidium of the Russian Academy of Sciences "Solar Activity and Physical processes in the Sun–Earth System," and the basic-research program of the Division of Physical Sciences of the Russian Academy of Sciences "Plasma Heliophysics."

REFERENCES

1. J. Sakai and C. De Jager, Space Sci. Rev. **77**, 1 (1996).
2. B. N. Dwivedi, H. S. Hudson, S. R. Kane, and Z. Svestka, Sol. Phys. **90**, 331 (1984).
3. R. A. Kopp and G. W. Pneuman, Sol. Phys. **50**, 85 (1976).
4. E. Priest and T. Forbes, *Magnetic Reconnection* (Cambridge Univ. Press, Cambridge, 2000; Nauka, Moscow, 2005).
5. A. N. Shakhovskaya and M. A. Livshits, Izv. Krym. Astrofiz. Obs. **102** (2006).
6. A. N. Babin, Izv. Krym. Astrofiz. Obs. **52**, 79 (1974).
7. A. N. Babin and A. N. Koval', Izv. Krym. Astrofiz. Obs. **73**, 3 (1985).
8. A. N. Shakhovskaya, V. I. Abramenko, V. B. Yurchyshyn, Sol. Phys. **207**, 369 (2002).
9. B. N. Handy, L. W. Acton, C. C. Kankelborg, et al., Sol. Phys. **187**, 229 (1999).
10. J.-P. Delaboudinière, G. E. Artzner, J. Brunaud, et al., Sol. Phys. **162**, 291 (1995).
11. I. M. Chertok and V. V. Grechnev, Astron. Zh. **80**, 162 (2003) [Astron. Rep. **47**, 139 (2003)].
12. I. M. Chertok and V. V. Grechnev, Sol. Phys. **229**, 95 (2005).
13. G. E. Brueckner, R. A. Howard, M. J. Koomen, et al., Sol. Phys. **162**, 357 (1995).
14. S. Yashiro, N. Gopalswamy, G. MicHαlek, et al., J. Geophys. Res. A **109**, 07105 (2004).
15. H. A. Garcia, Sol. Phys. **154**, 275 (1994).
16. P. H. Scherrer, R. S. Bogart, R. I. Bush, et al., Sol. Phys. **162**, 129 (1995).
17. M. A. Livshits and O. G. Badalyan, Astron. Zh. **81**, 1138 (2004) [Astron. Rep. **48**, 1037 (2004)].
18. G. A. Gary and R. L. Moore, Astrophys. J. **611**, 545 (2004).
19. Y. Liu, Y. Jiang, H. Ji, et al., Astrophys.J. **593**, L137 (2003).
20. L. K. Harra, P. Démoulin, C. H. Mandrini, et al., Astron. Astrophys. **438**, 1099 (2005).
21. M. A. Livshits and A. V. Belov, Astron. Zh. **81**, 732 (2004) [Astron. Rep. **48**, 665 (2004)].
22. O. G. Den, Astron. Zh. (2006) (in press).
23. Z. Mikic, J. A. Linker, V. Titov, et al., in *Proceedings of the European Solar Physics Meeting 11: Modeling of CMEs Originating in Active Regions, Leuven, Belgium, 2005*.
24. M. A. Livshits, in *Interrelation Between Processes during Impulsive and Post-Eruptive Phases as It Can Be Traced from the CORONAS-F Data, RESIK–RHESSI–SPIRIT Workshop, Wroclaw, 2005*.
25. V. V. Grechnev, A. M. Uralov, V. G. Zandanov, et al., Publ. Astron. Soc. Jpn. **58**, 55 (2006).

Translated by A. Getling